Hepatitis B virus replication is blocked by a 2-hydroxyisoquinoline-1,3(2H,4H)-dione (HID) inhibitor of the viral ribonuclease H activity

Catherine W. Cai [a,1], Elena Lomonosova [a,b,1], Eileen A. Moran [a], Xiaohong Cheng [a], Kunjan B. Patel [a], Fabrice Bailly [c], Philippe Cotelle [c], Marvin J. Meyers [d], John E. Tavis [a,b,*]

[a] Department of Molecular Microbiology and Immunology, Saint Louis University, 1100 S. Grand Blvd., Saint Louis, MO 63104, USA
[b] Saint Louis University Liver Center, Saint Louis University, 1100 S. Grand Blvd., Saint Louis, MO 63104, USA
[c] Chimie Moléculaire et Formulation, EA 4478 CMF, Université de Lille 1/ENSCL, 59655 Villeneuve d'Ascq, France
[d] Center for World Health and Medicine, Saint Louis University, 1100 S. Grand Blvd., Saint Louis, MO 63104, USA

ABSTRACT

Nucleos(t)ide analog drugs profoundly suppress Hepatitis B virus (HBV) replication but rarely cure the infection, so therapy is usually life-long. The nucleos(t)ide analogs inhibit the viral DNA polymerase and often push HBV to the brink of extinction, so it may be possible to eradicate HBV by suppressing HBV replication further. The HBV ribonuclease H (RNaseH) is a logical new drug target because it is the second of only two viral enzymes essential for viral replication. We recently developed a low through-put screening pipeline for inhibitors of the HBV RNaseH and viral replication. Here, we screened a series of twenty-three nitrogen-based polyoxygenated heterocycles including sixteen 2-hydroxyisoquinoline-1,3(2H,4H)-dione derivatives for anti-HBV RNaseH activity. Nine compounds inhibited the HBV RNaseH, but activity was marginal for eight of them. Compound #1 [2-hydroxyisoquinoline-1,3(2H,4H)-dione, HID] was the best hit with an IC_{50} of 28.1 μM and an EC_{50} of 4.2 μM. It preferentially suppressed accumulation of the viral plus-polarity DNA strand in replication inhibition assays, indicating that replication was blocked due to suppression of HBV RNaseH activity. It had a CC_{50} of 75 μM, yielding a therapeutic index of ∼18. The EC_{50} value was 7-fold lower than the IC_{50}, possibly due to cellular retention or metabolism of the compound, or higher affinity for the full-length enzyme than the recombinant form used for screening. These data indicate that the 2-hydroxyisoquinoline-1,3(2H,4H)-diones will have different structure–activity relationships for the HBV and HIV RNaseHs. Therefore, HID compounds may provide a foundation for development of more effective RNaseH inhibitors of HBV replication.

© 2014 Elsevier B.V. All rights reserved.

1. Introduction

Hepatitis B virus (HBV) infection causes chronic hepatitis B (CHB), an inflammatory liver disease that affects up to 350 million people world-wide. CHB causes >600,000 deaths each year due to cirrhosis, liver failure, and hepatocellular carcinoma (Ganem and Prince, 2004; Gerlich, 2013; Sorrell et al., 2009).

CHB is primarily treated with nucleos(t)ide analogs (Kwon and Lok, 2011; Sorrell et al., 2009). These drugs can reduce viral titers by 4–5 $\log_{10}$, often to below the limit of clinical detection (Marcellin et al., 2008; van Bommel et al., 2010; Woo et al., 2010). However, only a few patients clear the virus as measured by disappearance of the HBV surface antigen (HBsAg) from serum and the rise of anti-HBsAg antibodies (Block et al., 2013; Woo et al., 2010; Wursthorn et al., 2010). Although the rate of seroconversion in patients on nucleos(t)ide analog therapy is higher than in

untreated patients (Gish et al., 2010), the overwhelming majority remain chronically infected and dependent upon drug regimens costing up to $600 per month (Buti et al., 2009; Toy, 2013). Achieving higher rates of HBV clearance will thus necessitate development of new therapies that will probably be used in combination with the nucleos(t)ides to augment antiviral efficacy and drive the virus to extinction (Tavis et al., 2013b).

HBV replicates by reverse transcription catalyzed by the viral polymerase protein, which has two enzymatic activities in different domains. The DNA polymerase synthesizes the viral DNA and is the target of the nucleos(t)ide analogs (Ghany and Liang, 2007). The ribonuclease H (RNaseH) degrades the viral RNA after it has been copied into the minus-polarity DNA strand to permit synthesis of the viral plus-polarity DNA strand. The RNaseH is not targeted by existing drugs primarily due to difficulties in establishing screening assays. We recently developed a low-throughput screening pipeline for HBV RNaseH inhibitors (Hu et al., 2013; Tavis et al., 2013a), opening the door to anti-RNaseH drug discovery.

Many inhibitors of the HIV RNaseH have been identified (Ilina et al., 2012; Klumpp and Mirzadegan, 2006; Tramontano and Di Santo, 2010; Yu et al., 2008). We previously demonstrated that >20% of compounds selected for the ability to suppress the HIV RNaseH suppress the HBV enzyme, and found that a napthyridinone derivative (compound #12; structures are in Fig. 1) and β-thujaplicinol (compound #46) can suppress viral replication in cells by inhibiting the viral RNaseH (Hu et al., 2013; Tavis et al., 2013a). Here, we analyzed 2-hydroxyisoquinoline-1,3(2H,4H)-dione (HID) derivatives (Billamboz et al., 2008, 2011a, 2011b, 2013; Desimmie et al., 2013; Hang et al., 2004; Klumpp et al., 2003; Suchaud et al., 2014) and structurally related compounds for their ability to inhibit HBV RNaseH activity and viral replication based on the ability of this compound class to inhibit the HIV enzyme, with the goal of determining whether HID compounds may be suitable for development as anti-HBV drugs.

2. Materials and methods

2.1. Compound acquisition and synthesis

Compounds (Table 1 and Fig. 1) were acquired commercially or were synthesized according to previously reported methods [#78 (Billamboz et al., 2008); #79–80 (Billamboz et al., 2011a); #81 (Billamboz et al., 2011b); #82–85 and #90–91 (Billamboz et al., 2013); #86–89 (Suchaud et al., 2014)]. The synthetic methods and compound characterizations are described in the supporting information. All compounds were dissolved in dimethyl sulfoxide (DMSO) and stored at −80 °C.

2.2. RNaseH expression and purification

HBV RNaseH and human RNaseH1 were expressed in *Escherichia coli*, partially purified by nickel-affinity chromatography, and stored in liquid nitrogen as described (Tavis et al., 2013a).

2.3. Oligonucleotide-directed RNA cleavage assay

Oligonucleotide-directed RNA cleavage assays were conducted as previously described (Hu et al., 2013; Tavis et al., 2013a). Briefly, a ^{32}P-labeled RNA was combined with a complementary DNA oligonucleotide or a non-complementary oligonucleotide. This substrate was incubated with RNaseH and test compounds in 50 mM Tris pH 8.0, 190 mM NaCl, 5 mM MgCl$_2$, 3.5 mM DTT, 0.05% NP40, 6% glycerol, and 1% DMSO at 42 °C for 90 min. The products were resolved by electrophoresis, detected by audioradiography,

and quantified using ImageJ. IC$_{50}$ values were calculated with GraphPad Prism.

2.4. HBV replication assay

HepDES19 cells contain a genotype D HBV genome under control of a tetracycline-repressible promoter (Guo et al., 2007). Cells (0.6×10^6) were seeded into 6-well plates and incubated in DMEM/F12, 10% fetal bovine serum (FBS), 1% penicillin/streptomycin (P/S) with 1 μl/ml tetracycline. Tetracycline was withdrawn after 24 h. Compound #1 was applied to duplicate wells 48 h later in culture medium containing a final DMSO concentration of 1%. Medium containing the compound was refreshed daily for the following two days. Cells were harvested and non-encapsidated nucleic acids were digested with micrococcal nuclease (New England Biolabs) as described (Hu et al., 2013). HBV DNA was purified from capsids using QIAamp Cador Pathogen Mini Kit according to the manufacturer's instructions (Qiagen) with proteinase K incubation overnight at 37 °C. TaqMan PCR was performed for 40 cycles at an annealing temperature of 60 °C. Primers and probe (IDT Inc.) for the plus-polarity strand were: 5′CATGAACAAGAGATGATTAGGCAGAG3′; 5′GGAGGCTGTAGGCATAAATTGG3′; 5′/56-FAM/CTGCGCACC/ZEN/AGCACCATGCA/3IABkFQ. Primers and probe for the minus-polarity strand were: 5′GCAGATGAGAAGGCACAGA3′; 5′CTTCTCCGTCTGCCGTT3′; 5′/56-FAM/AGTCCGCGT/ZEN/AAAGAGAGGTGCG/3IABkFQ.

2.5. Cytotoxicity assays

Ninety-six well plates were seeded with 1.0×10^4 HepDES19 cells per well and incubated in DMEM with 10% FBS plus 1% P/S, 1% non-essential amino acids, and 1% glutamine. Compound #1 was diluted in medium and applied to cells 24 h after plating, with each concentration tested in triplicate. Medium containing the compound was refreshed daily for the next two days. Thiazolyl blue tetrazolium bromide (MTT, Sigma) was added to 0.25 mg/ml, the cultures were incubated for 60 min, metabolites were solubilized in acidic isopropanol, and absorbance was read at 570 nM. Cytotoxicity was also measured under the same culture conditions using the CytoTox-Glo assay (Promega) as recommended by the manufacturer.

3. Results

3.1. Biochemical screening against the HBV RNaseH

Twenty-three HID or related compounds (Table 1 and Fig. 1) were screened for anti-HBV RNaseH activity. First, a qualitative primary screening assay was performed against recombinant genotype D HBV RNaseH, then a qualitative assay was conducted against a genotype C isolate, and finally IC$_{50}$ values were determined for select compounds against the genotype D and/or C enzymes. Screening employed an oligonucleotide-directed RNA cleavage assay (Fig. 2A) in which a 264 nucleotide long internally ^{32}P-labeled RNA is annealed to a 20 nucleotide complementary DNA oligonucleotide or a non-complementary oligonucleotide as a specificity control. This heteroduplex substrate is incubated with the RNaseH along with the test compounds, and the cleavage products are resolved by electrophoresis (Hu et al., 2013; Tavis et al., 2013a).

The compounds were employed at 60, 20, and 10 μM in the qualitative screens. Nine compounds had activity at ⩽60 μM against either the genotype D or C enzymes, but activity was very weak for eight of them. The only compound with substantial activity was #1 [2-hydroxyisoquinoline-1,3(2H,4H)-dione, HID], which
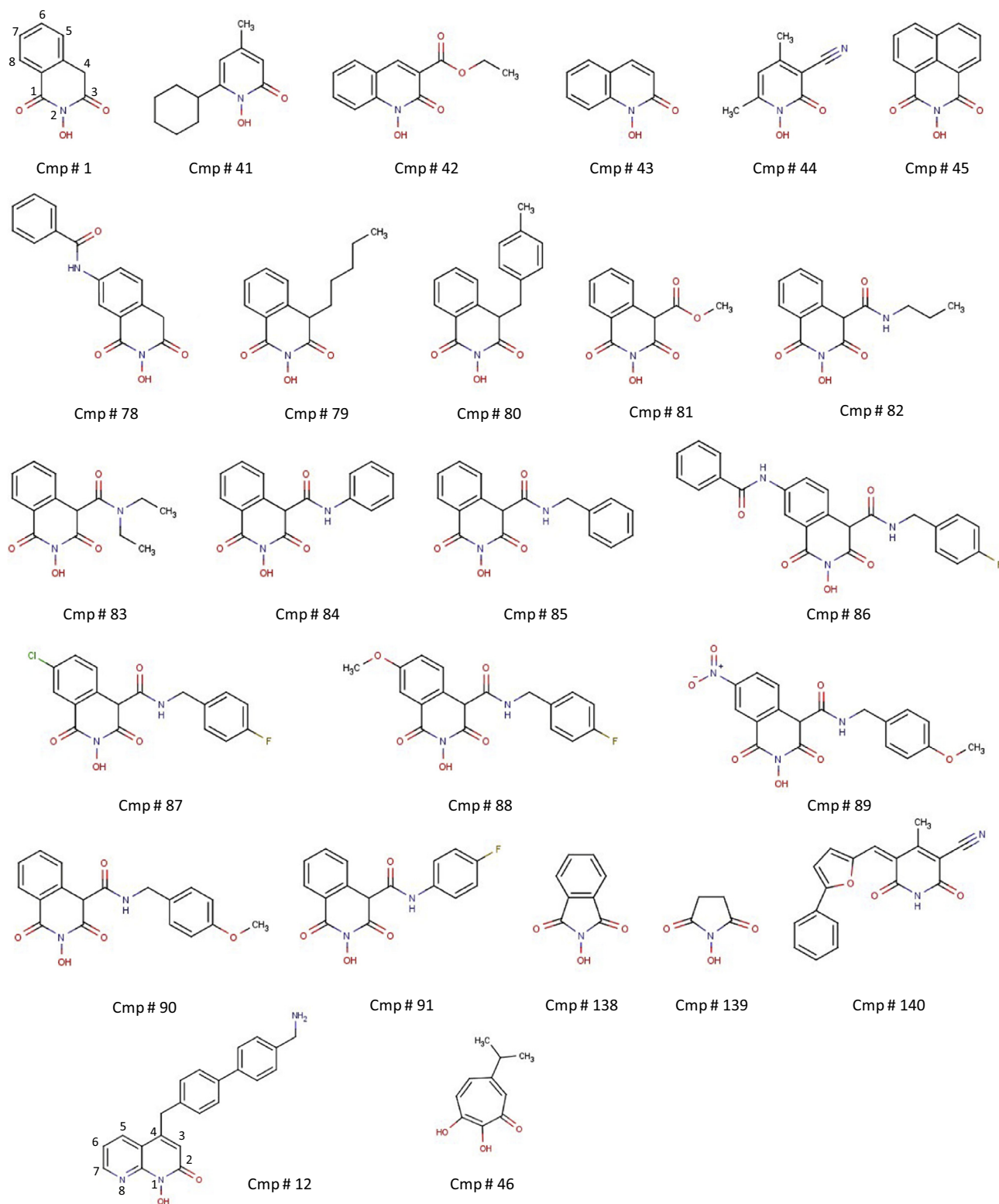
Fig. 1. Structures of the compounds used or discussed in this study.

inhibited both of the HBV enzyme at 10 μM (Table 1 and Fig. 2B). The potential for these results to be due to contamination of our enzyme extracts with *E. coli* RNaseH was excluded because compound #1 was inactive against the bacterial RNaseH (Fig. 2C). IC_{50} values were determined for compound #1 against both geno-

type D and C enzymes, and also against compounds #43–45, and 87 for comparison. Compound #1 had IC_{50} values of 28.1 ± 9.7 and 30.4 ± 12.9 μM against the genotype D and C enzymes, respectively, whereas IC_{50} values were >100 μM for the other compounds (Fig. 3 and Table 1).

Table 1
Biochemical screening results.

Compound number	Name[a]	Genotype D[b]	Genotype C[b]	Human RNaseH1[b]	Genotype D IC$_{50}$ (µM)	Genotype C IC$_{50}$ (µM)
1	TRC 939800	+++	+++	++	28.1 ± 9.7	30.4 ± 12.9
41	Ciclopirox	–	–	+		
42	Labotest 72543251	–	–	+		
43	Sigma PH008969	–	+	–		>100
44	Labotest 12243782	–	+	–		>100
45	TCI America H1040	–	+	–		>100
78	MB1	–	–	+		
79	MB2	–	–	–		
80	MB3	–	–	–		
81	MB4	–	–	+++		
82	MB71	–	+	+++		
83	MB88	+	–	+++		
84	MB105	+	–	+++		
85	MB103	+	–	+++		
86	VS42	+	–	+++		
87	VS55	–	–	+++	>100	
88	VS45	–	–	+++		
89	VS51	–	–	++		
90	MB104	–	–	++		
91	MB106	–	–	++		
138	Sigma H53704	–	–	–		
139	Sigma 130672	–	–	–		
140	Chembridge 6325462	–	–	++		

[a] Common name or manufacturer's product number.
[b] +, detectable inhibition at 60 µM; ++, inhibition at 20 µM; +++, inhibition at 10 µM; –, no inhibition.

3.2. Counter-screening against human RNaseH1

The compounds were counter-screened against recombinant human RNaseH1 in an initial effort to identify inhibitors with the least probability of being toxic. Thirteen compounds were active against the human enzyme at 10 or 20 µM, and two had activity at 60 µM (Table 1). The inhibition patterns differed between the HBV and human RNaseHs, with greater activity against the human enzyme usually being observed. Therefore, many HID compounds inhibited human RNaseH1, but the inhibition patterns against the HBV and human and RNaseHs were distinct.

3.3. HBV replication inhibition

Compound #1 was tested against HBV replication because it inhibited genotypes D and C RNaseHs well but had only moderate activity against human RNaseH1. Inhibiting the HBV RNaseH during viral replication suppresses production of the viral positive-polarity DNA strand and causes truncation of many minus-polarity DNA strands (Chen et al., 1994; Hu et al., 2013; Tavis et al., 2013a). Therefore, we employed strand-preferential quantitative PCR to measure accumulation of each viral DNA strand in the presence of compound #1 (Fig. 4A). In this assay, plus-polarity DNA preferential PCR depends upon amplification of the viral DNA across the gap in the minus-polarity DNA strand. Minus-polarity DNA preferential PCR depends on placing the amplification primers just upstream of the start site for the plus-polarity strand; this detects few plus-polarity strands because most plus-strand DNAs are shorter than full length (Tavis and Badtke, 2009). Fig. 4B demonstrates that the plus- and minus-polarity preferential PCR primers detected double-stranded HBV DNA with equal efficiency.

HBV replication was measured in HepDES19 cells (Guo et al., 2007), which are HepG2 cells stably transfected with a HBV genotype D genome under control of a tetracycline-repressible promoter. HBV induction kinetics were established by withdrawing tetracycline from the medium and harvesting intracellular capsid particles over the next 6 days. The cytoplasmic extracts containing the capsid particles were treated with micrococcal nuclease to destroy contaminating chromosomal DNA, the viral DNAs were released from the capsid particles by proteinase K digestion, and then the amount of plus-polarity HBV DNA recovered within the capsids was measured by quantitative PCR (Fig. 4C). Control experiments in which the PCR reactions were done without releasing DNA from the capsid particles failed to detect HBV DNA, confirming that the DNAs detected were derived from the HBV capsids (data not shown). Newly synthesized HBV DNA became detectable 3 days after withdrawal of tetracycline from the medium, and sufficient viral DNA to support reliable quantification of HBV replication accumulated by 5 days after withdrawal of tetracycline.

To measure the effect of compound #1 on HBV replication, HepDES19 cells were incubated for two days without tetracycline to initiate HBV replication. The cultures were then treated with compound #1 for three additional days, with provision of fresh medium plus compound every 24 h. HBV DNAs were purified from viral capsids and viral DNA levels were measured by quantitative PCR. Compound #1 suppressed HBV replication in qualitative replication inhibition assays at 60, 20, and 10 µM (Table 2). Quantitative assays revealed an EC$_{50}$ of 4.2 ± 1.4 µM against plus-polarity HBV DNA (Fig. 4D). The minus-polarity DNA strand in the same samples was not suppressed by treatment with compound #1; rather, its accumulation was somewhat enhanced. Therefore, synthesis of mature HBV genomes was suppressed by compound #1 via inhibition of the viral RNaseH activity.

3.4. Toxicity

Cytotoxicity of compound #1 was assessed in HepDES19 cells using an MTT assay under culture conditions analogous to those used for the replication inhibition assays (Fig. 5) or by measuring cell rupture (Table 2). CC$_{50}$ values were 74.7 ± 24 and 87 µM by the MTT and cell-rupture assays, respectively. These values were much higher than the EC$_{50}$ for compound #1, leading to a therapeutic index (TI) of 17.8.

4. Discussion

Screening compound classes known to suppress HIV RNaseH activity previously led us to identify a napthyridinone derivative
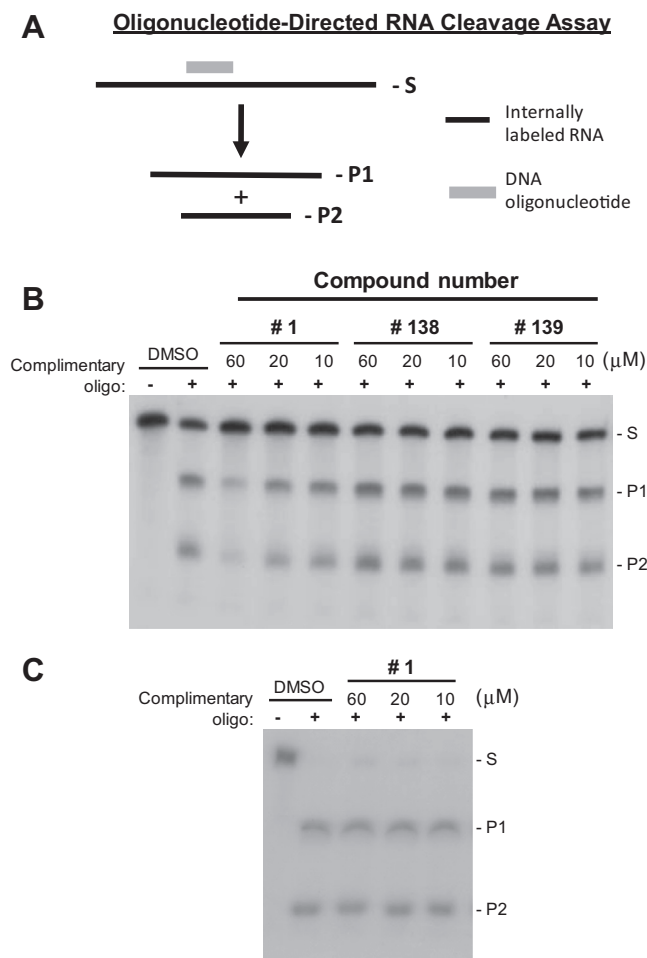
A

B

C

Fig. 2. Representative primary biochemical screening assays for the HBV RNaseH. (A) The oligonucleotide-directed RNaseH assay. Internally radiolabeled RNA is bound to a complementary DNA oligonucleotide, and the RNaseH cleaves the RNA within the DNA:RNA heteroduplexes. RNA, black line; DNA, grey line; S, RNA substrate; P1 and P2, RNaseH cleavage products. (B) Representative primary screening assay employing HBV genotype D RNaseH. DMSO, vehicle control. (C) *E. coli* RNaseH activity was not affected by compound #1 in the oligonucleotide-directed cleavage assay under identical conditions.

[compound #12 (Tavis et al., 2013a)] and β-thujaplicinol [compound #46 (Hu et al., 2013)] as inhibitors of HBV RNaseH activity and HBV genomic replication. Here, 15 HID compounds and 8 polyoxygenated nitrogen-containing heterocycles were screened against the HBV RNaseH. Eight very weak and one robust inhibitor were identified (Table 1).

The compounds were screened against HBV RNaseH enzymes from both genotypes C and D to maximize chances of finding hits with efficacy against genetically divergent HBV isolates. There was discord in efficacy of the compounds between the two genotypes for the weak inhibitors, but this was not surprising given that their activity was at the detection limit of our assays. However, compound #1 was equally effective against both genotype C and D enzymes (Table 1 and Fig. 3). Therefore, it is possible to identify HID compounds that can inhibit RNaseH enzymes from multiple HBV genotypes.

The compounds were counter-screened against human RNaseH1 as a first step toward eliminating compounds with unacceptable toxicity. Fifteen compounds inhibited the human RNaseH1, and many had robust activity at 10 μM (Table 1). Compound #1 was modestly active against the human RNaseH1, with detectable inhibition as low as 20 μM. Therefore, development of HIDs for use in
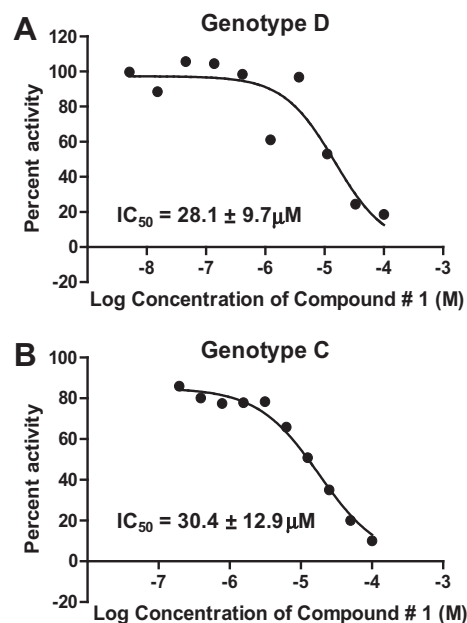
A

B

Fig. 3. Dose–response curves with compound #1 in the oligonucleotide-directed RNA cleavage assay against the HBV RNaseH. (A) Genotype D RNaseH. (B) Genotype C RNaseH. The curves are from representative assays. The numerical values are the average ± one standard deviation from three or four independent assays.

humans will require care to exploit structure–activity relationship (SAR) differences between the human and HBV RNaseH enzymes.

A previous study of the HID scaffold with substitutions at the 7-carbon position revealed widely varying degrees of inhibition of the HIV RNaseH (Billamboz et al., 2008). Inhibition of the HIV RNaseH did not predict inhibition of the HBV enzyme. For example, compound #1 has an IC_{50} of 5.9 μM against the HIV RNaseH (Billamboz et al., 2008, 2011b), which is ~5-fold lower than its efficacy against the HBV enzyme, while compound #81 strongly inhibits the HIV RNaseH (IC_{50} = 61 nM) (Billamboz et al., 2011b) but had negligible activity against the HBV enzyme (Table 1).

HID compounds inhibit the HIV RNaseH by chelating the active site divalent cations via interactions with the three oxygen atoms of the *N*-hydroxyimide function of the isoquinoline ring (Billamboz et al., 2011b; Klumpp et al., 2003). Our results are consistent with this mechanism also applying to the HBV RNaseH. Furthermore, the data establish four constraints on the SAR for HID compounds against the HBV enzyme. First, all three oxygens in the isoquinoline heterocycle appear to be needed for robust inhibition of the HBV enzyme. Compounds #41–44 lacking one keto function were poorly active against the HBV RNaseH. Second, the inactivity of compounds #138 and 139 against the HBV enzyme indicates that the nitrogen-containing six-member ring cannot be contracted to five atoms despite the apparent conservation of the metal-binding *N*-hydroxyimide function. This is similar to previous observations with influenza endonuclease inhibitors (Parkes et al., 2003). Third, introducing extended side chains at position 4 of the scaffold is detrimental (compounds #79–91), although compounds #83–86 showed weak inhibition of HBV genotype D at 60 μM. This is in contrast to the HIV RNaseH, in which some compounds displayed significant inhibition. For example, compound #79 had an IC_{50} of 13.2 μM (Billamboz et al., 2011a), and compounds #86 and 89 induced 41.2% and 67.2% inhibition at 10 μM, respectively (Suchaud et al., 2014). The discrepancy between HIV and HBV inhibition was even greater with the addition of an electron-withdrawing group such as a methoxycarbonyl moiety at position 4, which greatly bolstered anti-RNaseH activity of compound #81 against
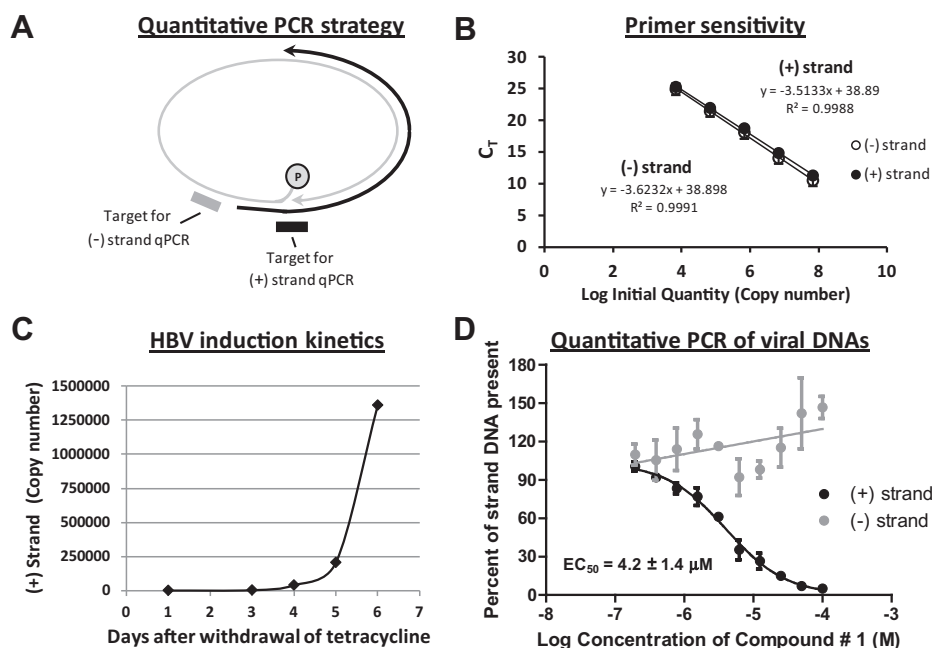
A

Quantitative PCR strategy

Target for
(-) strand qPCR

Target for
(+) strand qPCR

B

Primer sensitivity

(+) strand
$y = -3.5133x + 38.89$
$R^2 = 0.9988$

(-) strand
$y = -3.6232x + 38.898$
$R^2 = 0.9991$

○ (-) strand
● (+) strand

C

HBV induction kinetics

D

Quantitative PCR of viral DNAs

● (+) strand
● (-) strand

$EC_{50} = 4.2 \pm 1.4 \ \mu M$

Fig. 4. Effect of compound #1 on HBV replication. (A) Basis for the strand-preferential PCR reactions. The minus-polarity preferential primers/probe are upstream of the start site for the plus-polarity DNA, and the plus-polarity preferential primers/probe cross the gap in the minus-polarity DNA. Grey, minus-polarity DNA strand; black, plus-polarity strand; oval, the covalently-attached viral polymerase protein; arrows, 3′ ends of the DNAs. (B) Relative sensitivity of the plus- and minus-polarity preferential primers against a double-stranded HBV DNA template. A linear HBV DNA was serially diluted and used as a template for quantitative PCR employing the strand-preferential primers. Filled circles, plus-polarity preferential primers; open circles, minus-polarity preferential primers. Error bars are ± one standard deviation from three independent assays. (C) HBV induction kinetics in HepDES19 cells. Tetracycline was withdrawn from the medium, cytoplasmic HBV capsid particles were purified 1–6 days later, and plus-polarity HBV DNA derived from the capsid particles was measured by quantitative PCR. (D) Inhibition of HBV plus-polarity synthesis by compound #1. Viral nucleic acids were purified from cytoplasmic capsid particles from cells replicating HBV in the presence of varying concentrations of compound #1. Quantitative PCR preferential for plus- and minus-polarity strands of HBV DNA was performed to measure the effect of compound #1 on accumulation of plus- (black) and minus- (grey) strand HBV DNA. The results were normalized to the DMSO vehicle control. Data are the mean ± one standard error of the mean from three independent experiments each performed in duplicate.

Table 2
Inhibition of HBV replication by compound #1.

Replication inhibition[a]		Cytotoxicity[b]	
Qualitative	+++	MTT	74.7 ± 24
Quantitative	4.2 ± 1.4	Cell rupture	87

[a] +++, inhibition at $\leqslant 10 \ \mu M$ or CC_{50} (μM).
[b] CC_{50} (μM).

MTT assay
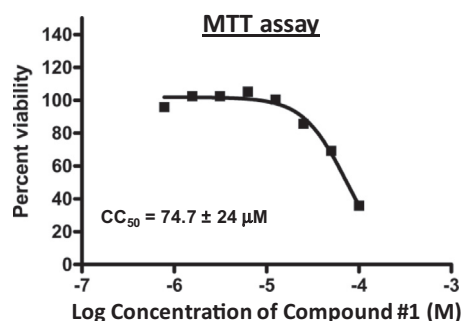

$CC_{50} = 74.7 \pm 24 \ \mu M$

Fig. 5. MTT toxicity assay for compound #1. An MTT assay was conducted in the presence of varying concentrations of compound #1 under culture conditions analogous to the replication assay in Fig. 4D. The curve is from a representative assay. The CC_{50} value is the average ± one standard deviation from three independent assays.

the HIV enzyme (Billamboz et al., 2011b). Finally, comparing compounds #1 and #45 reveals that joining positions 4 and 5 of the scaffold with a phenyl ring is not permissible. This supports a metal chelating mechanism for HBV RNase H inhibition similar to the HIV RNaseH and integrase mechanism. Indeed, we previously showed

that enolization of the keto function at position 3 is required for optimal magnesium chelation (Billamboz et al., 2011b), and this process is not possible for compound #45.

Only compound #1 met the criteria of our screening pipeline for assessment against HBV replication. It had an EC_{50} of $4.2 \pm 1.4 \ \mu M$ against replication of a genotype D HBV genome, compared to ~5 μM for β-thujaplicinol [compound #46, (Hu et al., 2013)] and <10 μM for the napthyridinone derivative [compound #12, (Tavis et al., 2013a)]. Suppressing HBV RNaseH activity blocks accumulation of the viral plus-polarity DNA strand (Chen et al., 1994; Hu et al., 2013; Tavis et al., 2013a). As predicted from the biochemical analyses, inhibition of HBV replication by compound #1 occurred by blocking the viral RNaseH activity because accumulation of the plus-polarity HBV DNA strand was strongly inhibited, while the minus-polarity DNA strand was not suppressed (Fig 4D). Moderate cytotoxicity was observed, with CC_{50} values of about 75 and 87 μM by the MTT and cell rupture assays, respectively (Table 2 and Fig. 5). This led to a TI of 17.8.

Compound #1 inhibited HBV replication at a ~7-fold lower concentration than it suppressed the HBV RNaseH in the biochemical assays ($EC_{50} = 4.2 \ \mu M$ vs. $IC_{50} = 28.1 \ \mu M$ for genotype D). This was unexpected given that the EC_{50} values for the other compounds that we have tested were similar or higher than their IC_{50} values [(Hu et al., 2013; Tavis et al., 2013a) and unpublished]. This could be due to cellular retention or metabolism of the compound, or to higher affinity for the full-length enzyme than the truncated recombinant form used for screening.

One HID compound, 2-hydroxy-4-methoxycarbonylisoquino-line-1,3(2H,4H)-dione [compound #81 in this paper = compound # 3 in (Billamboz et al., 2011b)], was previously found to inhibit HIV replication in MT-4 cells with an EC_{50} of 13.4 μM, presumably

by blocking the HIV RNaseH. However, several other HIDs did not clearly suppress HIV replication, in part due to toxicity. Thus, the EC_{50} values for most of these compounds against HIV, including compound #1, exceeded their CC_{50} values (Billamboz et al., 2008, 2011a, 2011b). This has precluded their development as anti-HIV agents.

Compound #1 shares some similarities to a napthyridinone compound that we previously reported to inhibit HBV replication (compound #12, Fig. 1) (Tavis et al., 2013a). They both display a bicyclic framework and a triad of metal chelating heteroatoms, but there are also major differences. First, the metal-chelating moiety is embedded into the bicyclic framework in the napthyridinone derivative since the N-8 nitrogen atom participates in metal chelation with the hydroxyl and keto functions at positions 1 and 2 (Fig. 1). In contrast, the three-oxygen metal-chelating moiety is located on a single ring in compound #1 (Fig. 1). Second, the orientation of the metal-chelating moieties relative to the aromatic ring is different. Third, there is a long side aminomethyldiphenylmethyl chain extending from the position 4 on the 1-hydroxy-1,8-naphthyridin-2(1H)-one ring. Thus, comparing compounds #1 and 12 may help guide development of an effective HBV RNaseH inhibitor. A crystal structure of the HBV RNaseH catalytic core would be very helpful for the design of catalytic inhibitors, but a structure is not available.

This series of HIDs showed that substitution of the scaffold at position 4 by alkyl groups and by ester and amide functions did not favor HBV RNaseH inhibition. The only potent compound was the unsubstituted compound #1, so other modifications of this hit, particularly on the aromatic ring, will be necessary to gain further insight into the SARs of the HID scaffold. Positioning a long side chain on the aromatic ring analogous to the naphthyridinone structure is an interesting possibility for pharmacomodulation.

As the design of clinically useful anti-RNaseH compounds becomes possible, so does the possibility of creating novel combination drug therapies for CHB that could suppress viral replication further than is currently possible in most patients. Combination therapy would be predicted to reduce the incidence of drug resistance seen with the inexpensive, older nucleos(t)ide such as lamivudine (Shaw et al., 2006; Zoulim and Locarnini, 2009). Therefore, development of RNaseH inhibitors could extend the time that the NAs remain effective. This could reduce the cost of treatment, which would be particularly important in the developing world where the bulk of CHB patients reside. However, the optimal outcome from development of anti-RNaseH drugs would be to devise a combination therapy that suppresses viral replication far enough to eradicate CHB. This would alleviate the immense health burdens imposed by HBV on the millions of afflicted people in the world.

Acknowledgments

Appendix A. Supplementary data

Supplementary data associated with this article can be found in the online version, at http://dx.doi.org/10.1016/j.antiviral.2014.05.007.

References

Billamboz, M., Bailly, F., Barreca, M.L., De, L.L., Mouscadet, J.F., Calmels, C., Andreola, M.L., Witvrouw, M., Christ, F., Debyser, Z., Cotelle, P., 2008. Design, synthesis, and biological evaluation of a series of 2-hydroxyisoquinoline-1,3(2H,4H)-diones as dual inhibitors of human immunodeficiency virus type 1 integrase and the reverse transcriptase RNase H domain. J. Med. Chem. 51, 7717–7730.

Billamboz, M., Bailly, F., Lion, C., Calmels, C., Andreola, M.L., Witvrouw, M., Christ, F., Debyser, Z., De Luca, L., Chimirri, A., Cotelle, P., 2011a. 2-hydroxyisoquinoline-1,3(2H,4H)-diones as inhibitors of HIV-1 integrase and reverse transcriptase RNase H domain: influence of the alkylation of position 4. Eur. J. Med. Chem. 46, 535–546.

Billamboz, M., Bailly, F., Lion, C., Touati, N., Vezin, H., Calmels, C., Andreola, M.L., Christ, F., Debyser, Z., Cotelle, P., 2011b. Magnesium chelating 2-hydroxyisoquinoline-1,3(2H,4H)-diones, as inhibitors of HIV-1 integrase and/or the HIV-1 reverse transcriptase ribonuclease H domain: discovery of a novel selective inhibitor of the ribonuclease H function. J. Med. Chem. 54, 1812–1824.

Billamboz, M., Suchaud, V., Bailly, F., Lion, C., Demeulemeester, J., Calmels, C., Andreola, M.L., Christ, F., Debyser, Z., Cotelle, P., 2013. 4-Substituted 2-hydroxyisoquinoline-1,3(2H,4H)-diones, as a novel class of HIV-1 integrase inhibitors. ACS. Med. Chem. Lett. 4, 606–611.

Block, T.M., Gish, R., Guo, H., Mehta, A., Cuconati, A., Thomas London, W., Guo, J.T., 2013. Chronic hepatitis B: what should be the goal for new therapies? Antiviral Res. 98, 27–34.

Buti, M., Brosa, M., Casado, M.A., Rueda, M., Esteban, R., 2009. Modeling the cost-effectiveness of different oral antiviral therapies in patients with chronic hepatitis B. J. Hepatol. 51, 640–646.

Chen, Y., Robinson, W.S., Marion, P.L., 1994. Selected mutations of the duck hepatitis B virus P gene RNase H domain affect both RNA packaging and priming of minus-strand DNA synthesis. J. Virol. 68, 5232–5238.

Desimmie, B.A., Demeulemeester, J., Suchaud, V., Taltynov, O., Billamboz, M., Lion, C., Bailly, F., Strelkov, S.V., Debyser, Z., Cotelle, P., Christ, F., 2013. 2-Hydroxyisoquinoline-1,3(2H,4H)-diones (HIDs), novel inhibitors of HIV integrase with a high barrier to resistance. ACS Chem. Biol. 8, 1187–1194.

Ganem, D., Prince, A.M., 2004. Hepatitis B virus infection–natural history and clinical consequences. N. Engl. J. Med. 350, 1118–1129.

Gerlich, W.H., 2013. Medical virology of hepatitis B: how it began and where we are now. Virol. J. 10, 239.

Ghany, M., Liang, T.J., 2007. Drug targets and molecular mechanisms of drug resistance in chronic hepatitis B. Gastroenterology 132, 1574–1585.

Gish, R.G., Chang, T.T., Lai, C.L., de Man, R., Gadano, A., Poordad, F., Yang, J., Brett-Smith, H., Tamez, R., 2010. Loss of HBsAg antigen during treatment with entecavir or lamivudine in nucleoside-naive HBeAg-positive patients with chronic hepatitis B. J. Viral Hepat. 17, 16–22.

Guo, H., Jiang, D., Zhou, T., Cuconati, A., Block, T.M., Guo, J.T., 2007. Characterization of the intracellular deproteinized relaxed circular DNA of hepatitis B virus: an intermediate of covalently closed circular DNA formation. J. Virol. 81, 12472–12484.

Hang, J.Q., Rajendran, S., Yang, Y., Li, Y., In, P.W., Overton, H., Parkes, K.E., Cammack, N., Martin, J.A., Klumpp, K., 2004. Activity of the isolated HIV RNase H domain and specific inhibition by N-hydroxyimides. Biochem. Biophys. Res. Commun. 317, 321–329.

Hu, Y., Cheng, X., Cao, F., Huang, A., Tavis, J.E., 2013. Beta-thujaplicinol inhibits hepatitis B virus replication by blocking the viral ribonuclease H activity. Antiviral Res. 99, 221–229.

Ilina, T., Labarge, K., Sarafianos, S.G., Ishima, R., Parniak, M.A., 2012. Inhibitors of HIV-1 reverse transcriptase-associated ribonuclease H activity. Biology 1, 521–541.

Klumpp, K., Hang, J.Q., Rajendran, S., Yang, Y., Derosier, A., Wong, K.I., Overton, H., Parkes, K.E., Cammack, N., Martin, J.A., 2003. Two-metal ion mechanism of RNA cleavage by HIV RNase H and mechanism-based design of selective HIV RNase H inhibitors. Nucleic Acids Res. 31, 6852–6859.

Klumpp, K., Mirzadegan, T., 2006. Recent progress in the design of small molecule inhibitors of HIV RNase H. Curr. Pharm. Des. 12, 1909–1922.

Kwon, H., Lok, A.S., 2011. Hepatitis B therapy. Nat. Rev. Gastroenterol. Hepatol. 8, 275–284.

Marcellin, P., Heathcote, E.J., Buti, M., Gane, E., De Man, R.A., Krastev, Z., Germanidis, G., Lee, S.S., Flisiak, R., Kaita, K., Manns, M., Kotzev, I., Tchernev, K., Buggisch, P., Weilert, F., Kurdas, O.O., Shiffman, M.L., Trinh, H., Washington, M.K., Sorbel, J., Anderson, J., Snow-Lampart, A., Mondou, E., Quinn, J., Rousseau, F., 2008. Tenofovir disoproxil fumarate versus adefovir dipivoxil for chronic hepatitis B. N. Engl. J. Med. 359, 2442–2455.

Parkes, K.E., Ermert, P., Fassler, J., Ives, J., Martin, J.A., Merrett, J.H., Obrecht, D., Williams, G., Klumpp, K., 2003. Use of a pharmacophore model to discover a new class of influenza endonuclease inhibitors. J. Med. Chem. 46, 1153–1164.

Shaw, T., Bartholomeusz, A., Locarnini, S., 2006. HBV drug resistance. mechanisms, detection and interpretation. J. Hepatol. 44, 593–606.

Sorrell, M.F., Belongia, E.A., Costa, J., Gareen, I.F., Grem, J.L., Inadomi, J.M., Kern, E.R., McHugh, J.A., Petersen, G.M., Rein, M.F., Strader, D.B., Trotter, H.T., 2009. National Institutes Of Health Consensus Development Conference Statement: management of hepatitis B. Ann. Intern. Med. 150, 104–110.

Suchaud, V., Bailly, F., Lion, C., Calmels, C., Andreola, M.L., Christ, F., Debyser, Z., Cotelle, P., 2014. Investigation of a novel series of 2-hydroxyisoquinoline-1,3-(2H,4H)-diones as human immunodeficiency virus type 1 integrase inhibitors. J. Med. Chem., http://dx.doi.org/10.1021/jm500109z.

Tavis, J.E., Badtke, M.P., 2009. Hepadnaviral genomic replication. In: Cameron, C.E., Götte, M., Raney, K.D. (Eds.), Viral Genome Replication. Springer Science+Business Media, LLC, New York, pp. 129–143.

Tavis, J.E., Cheng, X., Hu, Y., Totten, M., Cao, F., Michailidis, E., Aurora, R., Meyers, M.J., Jacobsen, E.J., Parniak, M.A., Sarafianos, S.G., 2013a. The hepatitis B virus ribonuclease H is sensitive to inhibitors of the human immunodeficiency virus ribonuclease H and integrase enzymes. PLoS Pathog. 9, e1003125.

Tavis, J.E., Gehring, A.J., Hu, Y., 2013b. How further suppression of virus replication could improve current HBV treatment. Expert Rev. Anti Infect. Ther. 11, 755–757.

Toy, M., 2013. Cost-effectiveness of viral hepatitis B & C treatment. Best Pract. Res. Clin. Gastroenterol. 27, 973–985.

Tramontano, E., Di Santo, R., 2010. HIV-1 RT-associated RNase H function inhibitors: recent advances in drug development. Curr. Med. Chem. 17, 2837–2853.

van Bommel, F., De Man, R.A., Wedemeyer, H., Deterding, K., Petersen, J., Buggisch, P., Erhardt, A., Huppe, D., Stein, K., Trojan, J., Sarrazin, C., Bocher, W.O., Spengler, U., Wasmuth, H.E., Reinders, J.G., Moller, B., Rhode, P., Feucht, H.H., Wiedenmann, B., Berg, T., 2010. Long-term efficacy of tenofovir monotherapy for hepatitis B virus-monoinfected patients after failure of nucleoside/nucleotide analogues. Hepatology 51, 73–80.

Woo, G., Tomlinson, G., Nishikawa, Y., Kowgier, M., Sherman, M., Wong, D.K., Pham, B., Ungar, W.J., Einarson, T.R., Heathcote, E.J., Krahn, M., 2010. Tenofovir and entecavir are the most effective antiviral agents for chronic hepatitis B: a systematic review and Bayesian meta-analyses. Gastroenterology 139, 1218–1229.

Wursthorn, K., Jung, M., Riva, A., Goodman, Z.D., Lopez, P., Bao, W., Manns, M.P., Wedemeyer, H., Naoumov, N.V., 2010. Kinetics of hepatitis B surface antigen decline during 3 years of telbivudine treatment in hepatitis B e antigen-positive patients. Hepatology 52, 1611–1620.

Yu, F., Liu, X., Zhan, P., De Clercq, E., 2008. Recent advances in the research of HIV-1 RNase H inhibitors. Mini Rev. Med. Chem. 8, 1243–1251.

Zoulim, F., Locarnini, S., 2009. Hepatitis B virus resistance to nucleos(t)ide analogues. Gastroenterology 137, 1593–1608.